HardwareX 16 (2023) e00490

Contents lists available at ScienceDirect

HardwareX

journal homepage: www.elsevier.com/locate/ohx

OpenASAP: An affordable 3D printed atmospheric solids analysis probe (ASAP) mass spectrometry system for direct analysis of solid and liquid samples

Robert Samples [a,*], Riko Mukoyama [a], Jacob Shaffer [b], Jill Mikucki [b], Lesley-Ann Giddings [a]

[a] Biochemistry Program, Smith College, 100 Green St Northampton, MA 01063, USA
[b] Department of Microbiology, University of Tennessee at Knoxville, Knoxville, TN 37902, USA

ARTICLE INFO

Keywords:
Mass Spectrometry
Atmospheric Solids Analysis Probe
Ambient ionization

ABSTRACT

Atmospheric Solids Analysis Probe (ASAP) mass spectrometry is a versatile technique allowing direct sampling of solid and liquid samples, but its adoption is limited due to the high cost of commercial ASAP systems. To address this, we present OpenASAP, an open-source ASAP system for mass spectrometers that can be fabricated for $20 or less using 3D-printing. Our design is readily adaptable to instruments from different manufacturers and can be produced with a variety of additive manufacturing techniques on consumer-grade 3D-printers. The probe allows for rapid sampling of solid and liquid samples without sample preparation, making it useful for high throughput screening, investigating spatial localization and function of analytes in biological samples, and incorporating mass spectrometry in instructional settings. We demonstrate its effectiveness by obtaining mass spectra of three natural product standards at levels as low as 10 ng/ml in liquid samples, and detecting these metabolites in microbial cultures that are difficult to analyze due to complex sample matrices or analyte properties. Furthermore, we demonstrate direct sampling of thin layer chromatography (TLC) spots of these cultures.

Specifications table

Hardware name	OpenASAP
Subject area	● Chemistry and biochemistry ● Biological sciences (e.g., microbiology and biochemistry) ● Environmental, planetary and agricultural sciences ● Educational tools and open source alternatives to existing infrastructure
Hardware type	● Measuring physical properties and in-lab sensors ● Biological sample handling and preparation
Closest commercial analog	Waters ASAP ProbeWaters RadianIonSense ASAP SystemAdvion Expression
Open source license	GNU General Public License (GPL)
Cost of hardware	$2.50–68
Source file repository	https://doi.org/10.5281/zenodo.8173130
OSHWA certification UID	US002380

* Corresponding author.
E-mail address: rsamples@smith.edu (R. Samples).

https://doi.org/10.1016/j.ohx.2023.e00490
Received 23 July 2023; Received in revised form 29 September 2023; Accepted 10 November 2023
Available online 17 November 2023

Hardware in context

Mass Spectrometry (MS) has proven to be an indispensable tool in analysis of complex mixtures and trace analytes in the biological and chemical sciences. [1] However, the most commonly used methods of introducing analytes into the mass spectrometer, including gas chromatography (GC–MS), liquid chromatography (LC-MS), and direct injection, require time consuming liquid sample preparation. [2] These methods can also introduce nonvolatile salts and detergents that may interfere with sample analysis [3] or be deposited in a gas chromatography column or mass spectrometer. [4] These limitations reduce the utility of MS in situations where rapid sampling of crude materials is desired.

To overcome these limitations, several atmospheric ionization techniques have been developed with varying ranges of applications, analyte coverage, sample preparation requirements, and cost. [5] These ambient ionization methods involve direct sampling and ionization of analytes. [5] One of the simplest atmospheric ionization techniques is the Atmospheric Solids Analysis Probe (ASAP), [6] which is a peripheral device used in MS to allow rapid probe-based sampling of solids and liquids in conjunction with an Atmospheric Pressure Chemical Ionization (APCI) source. ASAP probes typically consist of a handle into which a thermostable and electrically insulating single-use sampling capillary can be inserted. [7] A small quantity of solid or liquid sample can be collected on the surface of the capillary, which can be inserted into a port in the mass spectrometer source housing that positions the capillary between the mass spectrometer inlet and the APCI source. The position of the capillary enables analytes to be volatilized and ionized by the heated nitrogen plasma emitted by the APCI source. ASAP-MS has performed favorably in published studies comparing it with DART (Direct Analysis in Real Time) and conventional LC-MS methods. [8].

While commercial ASAP systems are available as peripheral devices or dedicated instruments, they are costly and limited to specific instruments. ASAP packages produced by Waters Technology Corporation (Saugus, MA) cost over $10,000 [9] and are only available for use with their instruments. [10] ASAP add-ons produced by IonSense are available for $5,000–10,000 and can be used with a wider range of instruments. [11] Dedicated ASAP instruments typically have a lower mass resolution, smaller footprint, and lower purchase price than high resolution instruments that peripheral ASAP systems are developed for. The Waters (Milford, MA) RADIAN System costs $62,000, [9] and the Advion (Lansing, NY) Expression with ASAP option costs $75,000 (Kevin Shea, personal communication, September 14, 2023). These costs may be hard to justify for those investigating the technique. To address these challenges, we present OpenASAP, an open source ASAP probe for Thermo Scientific instruments that can be manufactured on a wide range of consumer and industrial 3D-printers. We have validated the OpenASAP system for detecting a variety of complex natural product standards at concentrations as low as 10 pg/ml. Additionally, we demonstrate the detection of these molecules in unprocessed microbial cultures with complex matrices and show the utility of the OpenASAP system in downstream processing of microbial extracts through direct analysis of thin layer chromatography (TLC) spots of these extracts.

3D-Printing has been used to produce a variety of analyte delivery, ionization, and ion manipulation devices for mass spectrometry. [12] For example, several 3D-printed drift tube designs have been published adding ion mobility separation functionality to an existing mass spectrometer. [13–15] Ambient ionization has been a particular focus, [16] with the development of 3D-printed devices for paper [17] and cone spray [18,19] ionization, low temperature plasma ionization, [20] nebulized nanospray devices for single cell analysis, [21] and an MS interface for digital microfluidics. [22] 3D-printing has also been used to couple ambient ionization techniques with a motion system for imaging mass spectrometry with commercial Desorption Electrospray Ionization (DESI) sprayers [23] and 3D-printed low temperature plasma sources. [24].

Here, we have validated the OpenASAP system for detecting a variety of complex natural product standards at concentrations as low as 10 pg/ml. Additionally, we demonstrate the detection of these molecules in unprocessed microbial cultures with complex matrices and show the utility of the OpenASAP system in downstream processing of microbial extracts through direct analysis of TLC spots of these extracts. Current 3D-printed devices for mass spectrometry typically do not involve the thermally-demanding conditions involved in APCI and ASAP sampling, thus the suitability of 3D-printed components for these applications was unclear. Here we have implemented the OpenASAP system on a large high-resolution instrument. However, our finding that consumer grade materials and equipment can survive harsh conditions opens the door for further development of peripherals for field-operable instruments and

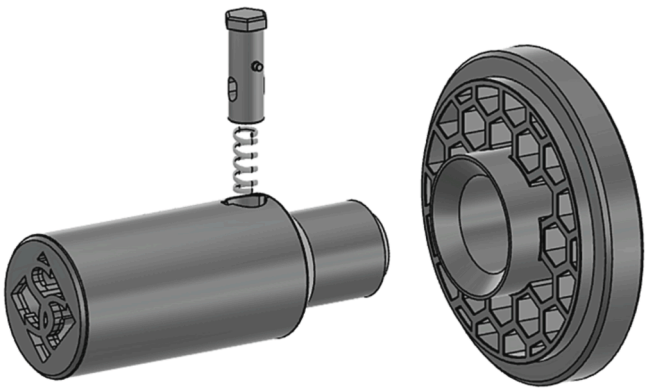

Fig. 1. Exploded Diagram of the OpenASAP probe and port.

lower-cost mass spectrometers in teaching applications.

We hope that the OpenASAP system will facilitate adaptation for a wide range of instruments and increase the accessibility of ASAP-MS to diverse users. By providing a low-cost alternative to commercial ASAP systems, this technology can be utilized by a broader range of researchers, potentially leading to new discoveries and advancements in the field.

Hardware description

The OpenASAP system (Fig. 1) builds on the design of published ASAP systems and has similar functionality and sampling time when compared to commercial ASAP devices. [11,25] Existing ASAP systems can be categorized into two designs. The simplest design, used by Advion [26] (Lansing, NY), Waters RADIAN, [27] and IonSense [11] ASAP systems, involves the use of a probe to position a sampling capillary between the MS inlet and APCI source, which facilitates analyte desorption from the capillary by the heated nitrogen plasma stream. [25] The more complex design used by Waters ASAP peripheral upgrades involves inserting the probe and sampling capillary into a channel in the APCI source so that the plasma stream flows past the entire sampling surface. While this approach may have benefits, such as ensuring the entire sampling surface is exposed to desorption gas, more homogeneous flow dynamics, and uniform desorption of analytes, it is more technically challenging and cannot be retrofitted to existing APCI sources. Consequently, the OpenASAP probe is placed in a separate port on the MS source housing rather than in the APCI source itself, as in the case of the Waters system.

The OpenASAP system is composed of the following three 3D-printed components: a probe port retrofitted to the existing MS source housing, a probe, and a probe button. Additionally, a 4 x 8 mm metal spring is required for capillary tensioning (Fig. 2). Sampling is performed using glass melting point capillaries (90 x 1.8 mm). Similar to existing systems, the probe provides an easy consumable handling mechanism. Existing ASAP systems, such as those produced by Advion, commonly employ a capillary handling system reminiscent of a micropipette. Due to the lack of additive manufacturing materials with both the flexibility and thermal resistance necessary for the capillary securing components to be in close proximity to high temperature nitrogen, the OpenASAP probe uses a spring-loaded locking mechanism on the side of the probe. The chamfered capillary hole in the probe ensures easy insertion of capillaries.

The OpenASAP system can be produced with a range of additive manufacturing techniques. Prototyping and fabrication was tested with fused deposition modeling (FDM), stereolithography (SLA), masked stereolithography (MSLA) printers ranging from consumer to industrial grade. However, it is preferable to use a high-temperature photopolymer resin or FDM filament, such as polyamide/nylon or polycarbonate. Initial prototyping was performed using PLA + on a consumer-grade FDM printer. The prototype showed only slight dimensional instability over several hours of testing. Later prototypes were printed in carbon fiber PLA, which was purchased for under $27/kg and annealed on the print bed to achieve high heat resistance without deformation. [28] Use of carbon fiber PLA followed by annealing allows the OpenASAP system to be fabricated on any consumer-grade unenclosed FDM printer with a hardened nozzle.

In contrast to commercial systems costing several thousand dollars, [9,11] the OpenASAP system can be fabricated for as little as $2.50 with consumer grade additive manufacturing equipment depending on equipment availability and material choice. It can be retrofitted to any Thermo Scientific (Waltham, MA) mass spectrometer with an IonMax source housing and APCI source and can be adapted to other instruments as well. Instrument and ion source housings well suited for adaptation of the OpenASAP system include those with removable windows for viewing the ion source or for installation of atmospheric pressure photoionization systems. Ionsense ASAP systems have been developed for Waters micromass instruments [11] however servo-driven lockspray baffle mechanisms on High Resolution Waters instruments may prove to be an obstacle. We believe adaption for Bruker instruments, Agilent Instruments, Sciex instruments with Turbo V Ion Sources, and Thermo instruments with the newer IonMax NG sources will be relatively

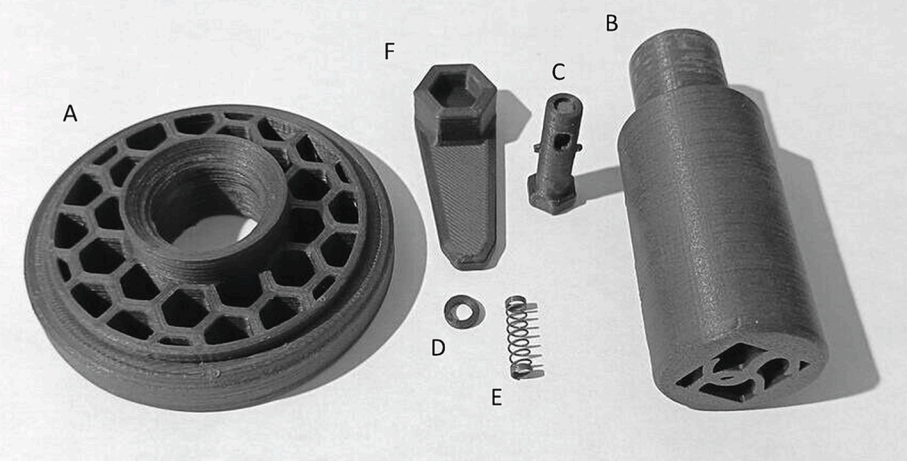

Fig. 2. Image of the parts required for assembly of the probe. A. Probe port B. Probe handle C. Probe button D. Probe spring spacer E. Probe spring F. Probe button wrench.

straightforward by altering the OpenASAP port and/or probe dimensions in CAD software to accommodate different window configurations and clearance.

- Lowers barrier to entry for probe-based sampling
- Allows rapid analysis of solids and liquids with no sample preparation required
- Adaptable to a wider range of instruments
- Easy to use probe using standard melting point capillaries with button release mechanism
- Under 30 s sampling time

Design files summary

Design file name	File type	Open source license	Location of the file
OpenASAP_IonMax_V1.step	STEP	GNU General Public License (GPL)	https://github.com/robertsamples/OpenASAP
Port.stl	STL	GNU General Public License (GPL)	https://github.com/robertsamples/OpenASAP
Button.stl	STL	GNU General Public License (GPL)	https://github.com/robertsamples/OpenASAP
Probe_body.stl	STL	GNU General Public License (GPL)	https://github.com/robertsamples/OpenASAP
Spacer.stl	STL	GNU General Public License (GPL)	https://github.com/robertsamples/OpenASAP
Wrench.stl	STL	GNU General Public License (GPL)	https://github.com/robertsamples/OpenASAP

3D models of the OpenASAP system parts are available in both STL format for 3D-printing and STEP format for modification in CAD software.

Bill of materials summary

Consumables

Designator	Component	Number	Cost per unit -currency	Total cost -currency	Source of materials	Material type
	4.25 x 18 mm or similar ballpoint pen compression spring	1	$0.25–1.00	$0.25–1.00		Metal
FDM Material Option	Tinmorry Carbon Fiber PLA	0.0675 kg	$27	$1.82	Amazon/ShenZhen Yaduo Trade Co., Ltd	Polymer
MSLA Material Option	Siraya Tech Sculpt Ultra or similar high temperature MSLA Resin	0.07 kg	$75	$5.25	Siraya Tech	Polymer
SLA Material Option	Formlabs Form 2 Tough 2000 Resin	0.075 L	$200	$15	Formlabs Inc.	Polymer
Compercial Printing Service	*MJF PA12 GF*			$68	Shapeways Inc.	Polymer

Equipment

Fabrication Type	Equipment	Example	Cost	Source of materials
FDM	*Printer*	Elegoo Neptune 3 Pro	$200	Shenzhen Elegoo Technology Co., Ltd.
	Nozzle	Mk8 Hardened Steel Nozzle	$10	Amazon
MSLA	*Printer*	Elegoo Mars 3 4 k	$155	Shenzhen Elegoo Technology Co., Ltd.
	Wash and cure system	Mercury Plus V2.0	$105	Shenzhen Elegoo Technology Co., Ltd.
	Wash solvent	*Isopropanol 4L*	$45	

We have tested fabrication of the OpenASAP system using FDM, MSLA, and SLA processes and have included the materials and cost for these options, however only one is required. Total cost of fabrication is estimated to be between $2.50 and $16 depending on material choice. If FDM printing with PLA is selected we suggest the use of either polycarbonate, PA/nylon, or annealed PLA (preferably a carbon fiber composite for dimensional stability during annealing) over ABS/ASA, PETG, or unannealed PLA due to the higher heat deflection temperature of the former materials. Thermal depolymerization of ABS/ASA may additionally increase background in MS spectra, although this has not been tested. Carbon fiber PLA is an excellent option for newcomers to additive manufacturing as it can be printed on any unenclosed entry level FDM printer with a hardened nozzle and can be annealed to achieve high heat resistance [28]. Resin printing with SirayaTech or similar resin will yield parts with PEEK-like properties but requires comparatively expensive

equipment and materials. We provide examples of suitable entry-level equipment suitable for fabrication of the OpenASAP system, alternatively parts may be purchased from a commercial printing service for $50–100. Total fabrication and installation time is 3–5 h, most of which is printing and annealing (in the case of CF-PLA).

Build instructions

A video of fabrication, installation, and use of the OpenASAP system can be viewed at https://github.com/robertsamples/OpenASAP.

3D-Printing

SLA/MSLA

Any resin intended for high temperature applications can be used according to the manufacturer's instructions. Here Siraya Tech Sculpt Ultra was printed with an Elegoo Mars 3 consumer MSLA printer with an initial resin temperature of 25–30 °C using 50-μm layer height, 2.4 s normal exposure time, 45 s bottom exposure time, and 5 bottom layers. Prints were washed for 10 min in 90 % isopropanol, immersed in water, and cured under UV light for 10 min. SLA printing on a Formlabs Form2 3D-Printer was also tested with Formlabs Tough 2000 resin. Appropriate PPE and safety precautions should be adhered to when using any resin printing process due to the toxicity of resins. These include adequate ventilation, use of a secondary enclosure around consumer resin printers to reduce VOC release, and use of an organics respirator when handling resin and uncured parts.

FDM

An FDM printer may be used with a material with an appropriately high heat deflection temperature such as nylon, polycarbonate, or annealed PLA according to the manufacturer's instructions. Here Tinmorry carbon fiber PLA (ShenZhen Yaduo Trade Co., Ltd., Shenzhen, China) was used on an Elegoo Neptune 3 consumer FDM printer with a 0.4 mm nozzle, 0.2 mm layer height, 4 perimeters, 40 % gyroid infill, and automatic organic supports generated by Prusaslicer 2.6 alpha 5 (Prusa Research, Prague, Czech Republic), was used. The parts were annealed for thirty minutes at 100 °C prior to assembly. When sanding carbon fiber PLA or similar composites a respirator must be worn and adequate ventilation used to limit exposure to small carbon fiber particles.

We recommend printing parts in the following orientation when using FDM. Orientation may be changed while using SLA/MSLA although we recommend printing the probe body in the pictured orientation (Fig. 3) or inverted 180 degrees, as the internal geometry has been optimized for printing in these directions.

Post-processing and assembly

Remove support material if applicable, removal of supports from the inside of the probe channel carefully using forceps or dental picks. If carbon fiber PLA is selected. annealing may be done in a laboratory oven, however we annealed parts using the printer heat bed. This was done by placing the parts on a 1-cm bed of gyroid infill printed with 3 walls and no top layers to allow airflow, covering the parts with a box made of 1-cm packing foam in which the 3D printer was shipped, and heating the bed to 100 °C for 30 min (Fig. 4).

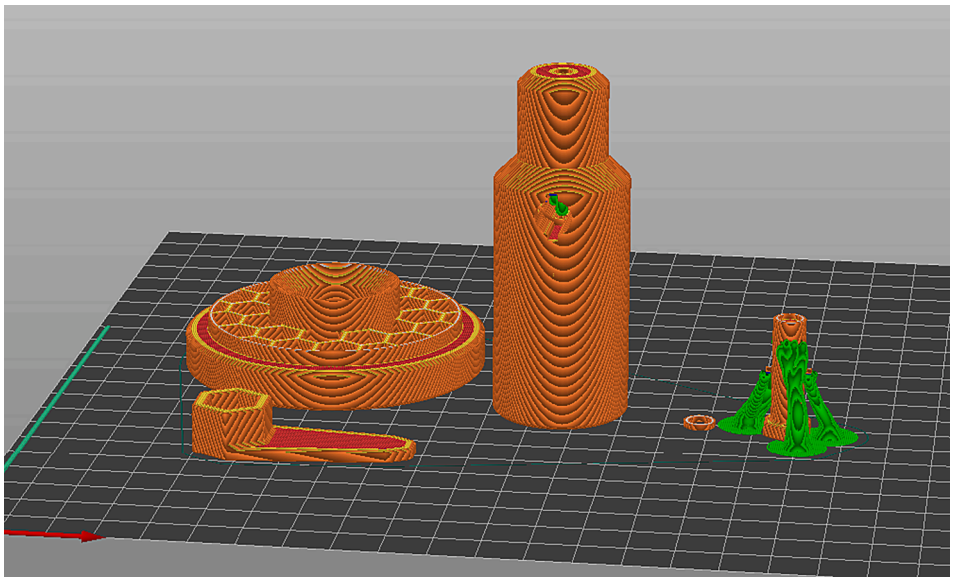

Fig. 3. Example of sliced parts in PrusaSlicer.

Parts were allowed to cool slowly to below the glass transition temperature of approximately 50 °C before being removed from the chamber. Corrections for any contraction and expansion of printed parts were done by printing a 20 mm calibration cube and measuring the X, Y, and Z dimensions before and after annealing. A 1 % contraction in X and Y dimensions and 2 % expansion in Z dimension were found and thus parts were scaled prior to slicing to compensate for these modifications. Scaling requirements may be significantly different depending on material selection and printing parameters.

Verify parts fit together properly. The button wrench should fit on the top of the button and allow it to be inserted into the button hole (Fig. 5).

When the probe button bottoms out, it should be turned ¼ turn clockwise to align guide cylinders on the side of the button with the travel channel (Fig. 6).

The button should move freely within the channel (Fig. 7). After this is tested, disassemble the button and probe. If parts do not fit together easily confirm all support material has been removed and lightly sand or file if needed. When sanding carbon fiber PLA a respirator is required due to the risks associated with this material.

Disassemble a retractable ballpoint pen or obtain a 4.25 × 18 mm or similar compression spring (Fig. 8). The spring shown here was obtained from a PaperMate InkJoy 300RT pen. The exact dimensions are not critical provided the probe button can reach the depth required to turn into the travel channel. A spring that is longer may be cut to length.

Confirm the spring length is sufficient to provide tension to the probe button while still allowing the button to be locked into the travel channel. To do this, the spring is placed in the recess of the button and the spring spacer is placed around the spring to prevent it from bending in the button hole (Fig. 9). The button is reinserted into the probe as before. If it does not bottom out and turn, try a different pen, or cut the spring to length. Complete the final reassembly of the probe. Although not required, we suggest using a drop of cyanoacrylate glue around the spring spacer and recess in the probe button to secure these to the spring.

Unscrew the four M2 screws securing the outer housing plate screws on the left side and top of the source housing, as well as the x alignment adjustment nut. Remove the M4 socket cap screw securing the source housing window side flange (Fig. 10).

Remove the flange and replace the acrylic window with printed port, then reassemble flange and housing plates (Fig. 11).

Install the IonMax source onto the MS interface and confirm that the tip of the capillary aligns with the MS inlet (Fig. 12).

Operation instructions

When operating the openASAP system, it is important to avoid contact with heated or electrically charged source components as they can reach high voltages and temperatures. We recommend always putting the mass spectrometer in standby mode when handling the source. Additionally, an electrically insulating material, such as glass, should be used for the sample collecting component of the probe.

Before using the openASAP system, the APCI source and corona discharge needle must be properly installed in the mass spectrometer housing following the manufacturer's instructions. For Thermo instruments, this involves inserting the APCI source and connecting the LEMO electrical connectors and fittings for auxiliary and sheath gas flow. The corona discharge needle should be inserted into the needle hole and the needle grub screw tightened to secure it. High voltage is supplied through a coaxial LEMO connection on the top of the source housing.

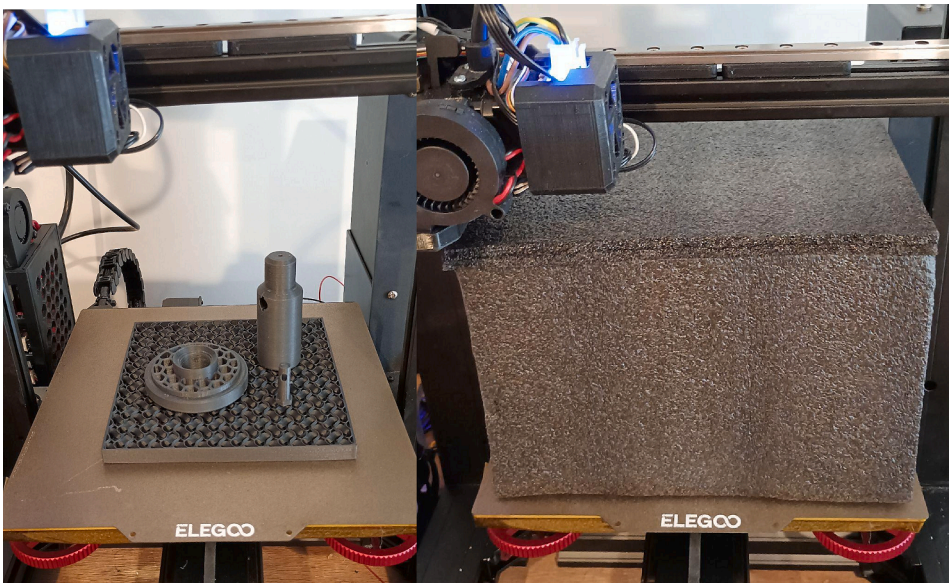

Fig. 4. *left.* Photo of probe parts on a bed of gyroid infill prior to annealing on the printbed. *right.* Photo of parts during annealing at 100 °C inside of an insulting box constructed from the foam used to protect the printer during shipping.

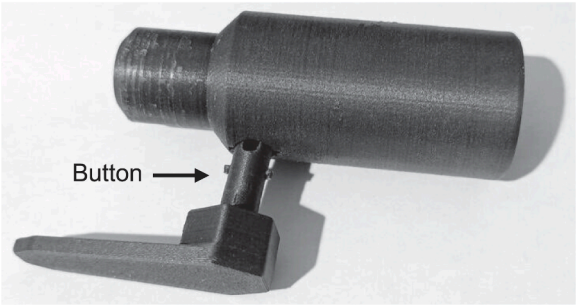

Fig. 5. Photo of the probe button being inserted.

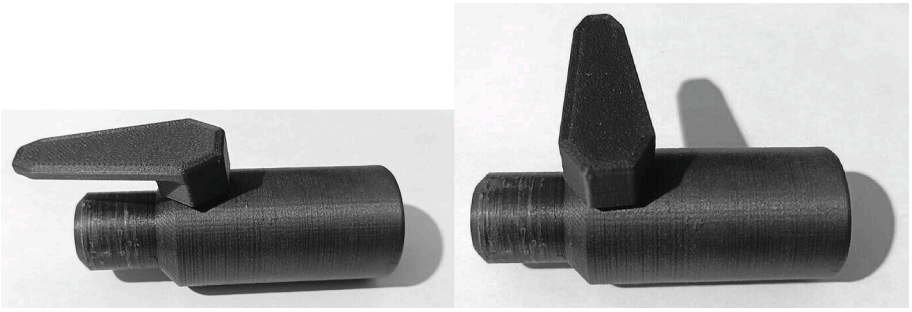

Fig. 6. Photo of the probe button being locked in place.

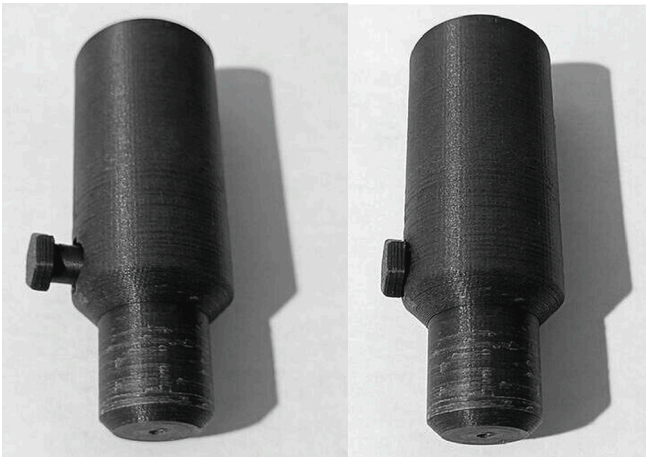

Fig. 7. Photo of the probe with button depressed and extended to check part clearance.

The APCI settings may need to be adjusted based on the analyte and instrument being used. For Thermo instruments, we recommend using the following settings as a starting point: Probe position C, a heater temperature of 325 °C, 5 μA current, and a sheath and auxiliary gas flow rate of 30 and 10 arbitrary units, respectively.

To load a capillary into the ASAP probe, depress the button and insert the capillary open end first until it reaches the maximum depth (Fig. 13).

Collect the sample on the probe tip and then insert it into the APCI source after starting a continuous or set duration acquisition (Fig. 14).

Observe the mass spectra as they are acquired. When the signal intensity diminishes as analytes are desorbed from the probe, end the acquisition and withdraw the probe from the source housing. Depress the button over a glass waste container to dispose of the capillary. In some cases where volatile analytes are completely desorbed by the nitrogen stream, the capillary may be reusable.

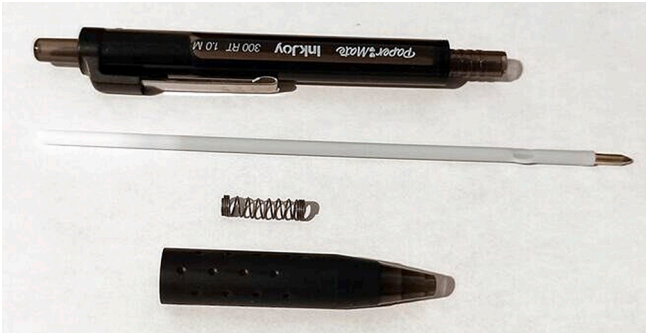

Fig. 8. Disassembled InkJoy 300 RT pen.

Fig. 9. Probe button, spring, and spacer after before final insertion into the probe body.

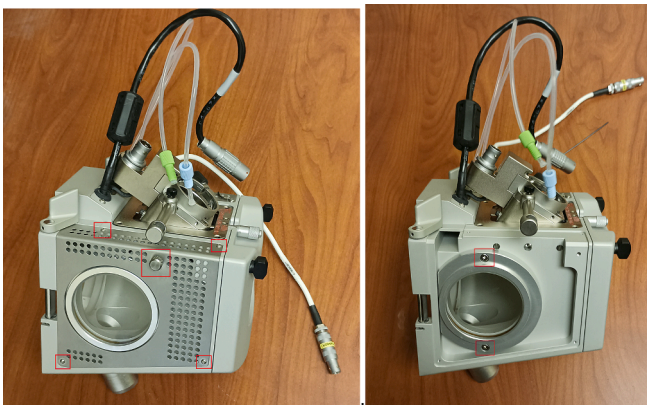

Fig. 10. Disassembly of the Thermo Scientific IonMax source housing window, with screw locations to be removed highlighted in red. (For interpretation of the references to colour in this figure legend, the reader is referred to the web version of this article.)

Validation and characterization

Data collection

Three microbial strains possessing biosynthetic gene clusters for the production of secondary metabolites with a range of different polarities and molecular weights were selected for validation studies. These included two Antarctic microbial strains, *Massilia frigida* strain DJPM01 [29] and *Arthrobacter* sp. strain FRX14, [30] which possess prodigiosin and ectoine gene clusters, respectively. Additionally, *Streptomyces alboflavus* (NRRL B-1273), a known tetracycline producer, [33] was included. Prodigiosin is a basic and highly aromatized compound [31] tetracycline is a moderately polar polyketide synthase product, [32] and ectoine is small zwitterionic and highly polar compound for which we have been unable to achieve acceptable retention with C18 columns (Fig. 20). These three strains were cultured for two weeks on solid media. *Streptomyces alboflavus* (NRRL B-1273) was cultured on ISP2 agar plates and incubated at 28 °C while the Antarctic strains were cultured on R2A (BD Difco, Franklin Lakes, NJ) agar plates at 15 °C. Diffusible yellow pigment was evident in *Streptomyces alboflavus* (NRRL B-1273) plates and non-diffusible red pigment was noted in *M. frigida* strain DJPM01 plates.

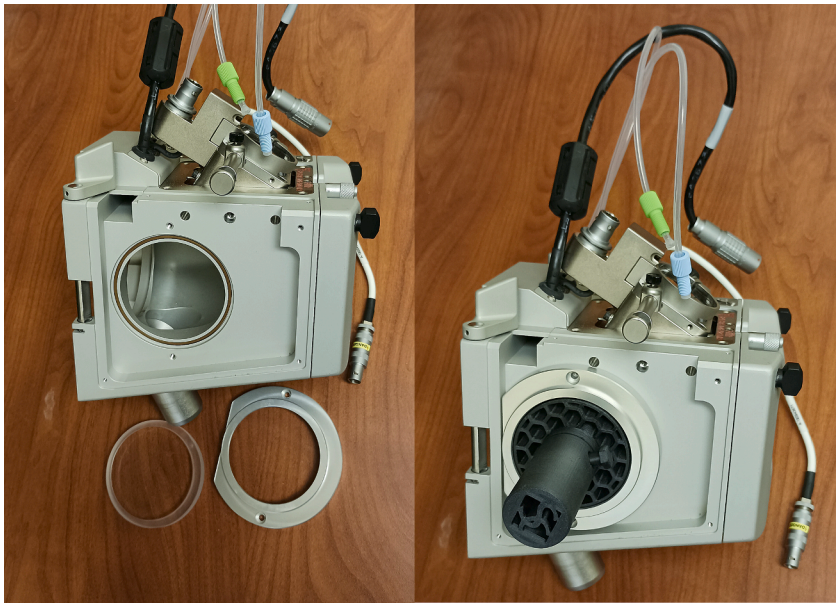

Fig. 11. IonMax source housing immediately before (left) and after (right) installation of the OpenASAP probe.

Fig. 12. *left.* IonMax source housing with APCI source and OpenASAP system installed and mounted on the Q Exactive HF-X. *right*. View of the MS inlet and source components showing the capillary in the OpenASAP system positioned between the APCI source and MS inlet.

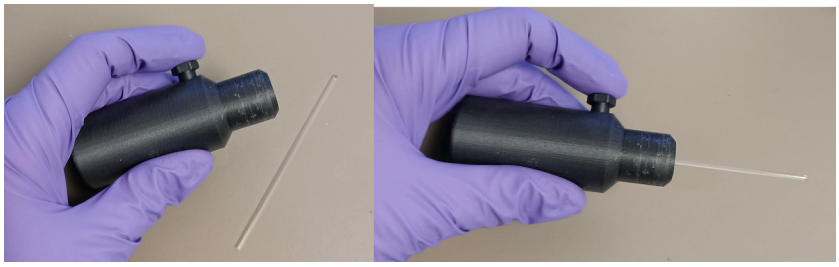

Fig. 13. Capillary insertion process.

Analytic standards of prodigiosin, ectoine, and tetracycline were purchased (Sigma-Aldrich; St. Louis, MO) and standard solutions ranging from 1×10^{-2}–10^{-14} g/mL were generated in 10-fold dilutions, 1×10^{-2} and 1×10^{-3} g/ml concentrations were excluded for prodigiosin as insufficient material was available. To determine the approximate limit of detection for these analytes, the ASAP capillary was inserted into 900 µl of each standard in a microcentrifuge tube and inserted into the probe port while data was acquired with the source parameters listed in the operation section, a SIM scan range from the exact mass of the M + H ion of the standard ± 2.5 Da, 30,000 resolution, 1e6 AGC target, and 50 ms max injection time. Extracted ion chromatograms for the precursor ion were generated using Thermo Scientific Freestyle software and the peak in the chromatogram view was integrated to determine the quantity

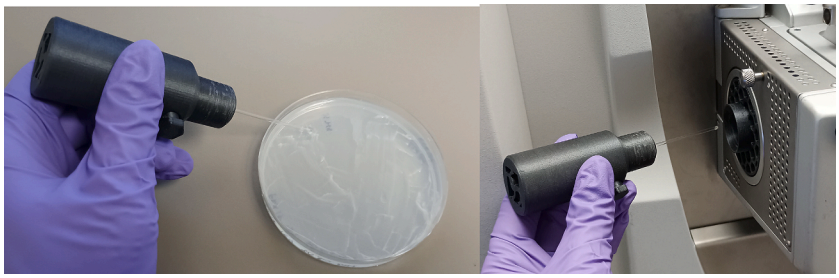

Fig. 14. *left*. Direct sampling of *Arthrobacter* sp. strain FRX14 on agar *right.* Insertion of the probe following sampling.

of standard detectable at each concentration and to generate a standard curve. In order to evaluate reproducibility, 1×10^{-5} g/ml solutions of each standard were sampled five times each and coefficient of variation calculated for each compound.

ASAP identification of these compounds in microbial cultures was conducted by by touching the probe to the surface of a colony then inserting the probe into the port as before using a SIM method. Sampling of the prodigiosin producer *M. frigida* strain DJPM01 was conducted in full scan mode with a 50–750 Da scan range as prodigiosin's *m/z* 324 for the [M + H] adduct was the base peak. After desorption was complete, a standard of a known concentration was collected on a new capillary and inserted to provide a reference within the same raw acquisition file. The experiment was repeated to acquire full scan MS spectra with a 50–750 Da scan range and MS/MS data with a 0.9 Da isolation window, 35 V NCE, and MS/MS mass range of 50–750 Da. These data were visualized in Thermo Freestyle. Extracted ion chromatograms for the targeted precursor masses were generated to view the quantity of analyte detected during insertion of the probe with microbial samples and standards.

To determine the volume of sample retained on the capillary, we used a spectrophotometer to measure the absorbance of the tetracycline standard curve. We sampled a concentrated tetracycline stock with the OpenASAP system and desorbed material from the capillary into 1 ml of methanol so that a dilution factor and sampling volume could be calculated. A standard curve of tetracycline from 3.125 to 100 μg/ml in methanol was prepared by serial dilution. One milliliter of a 10 mg/ml methanolic solution of tetracycline was directly sampled with the OpenASAP system and the collected material desorbed in 1 ml of methanol. Each standard (200 μl) and the desorbed solution were transferred to a 96-well plate in triplicate and the absorbance was measured at 300 nm. The tetracycline concentration of this solution was used to calculate the dilution factor from the sampled stock and thus the volume added.

To evaluate the OpenASAP system in downstream processing of samples or reaction mixtures and in screening, TLC was run on ethyl acetate extracts of *M. frigida* strain DJPM01 grown for 10 days on R2A media at 15 °C. [29] The ethyl acetate extract of *M. frigida* strain DJPM01 and prodigiosin were separately spotted on TLC plates, (10 x 10 cm aluminum backed 60 mesh F_{254} silica plates, Beijing Laikensi Technology Development Co. Ltd., Beijing, China) which were run with a 90:10:1 chloroform:methanol:formic acid mobile phase. The open end of the melting point capillary was used in the OpenASAP probe to scrape a small quantity of selected TLC spots and MS data was acquired as previously described with a full scan method (50–750 Da). Depending on the consistency of the stationary phase, spraying the plate with a small quantity of solvent or water prior to scraping helped at times. Previous work has used a similar procedure in which the TLC plate is scraped and a wetted probe dipped in the stationary phase. [34].

Results and discussion

The 3D-printed atmospheric analysis sampling probe (ASAP) peripheral was successfully integrated with a mass spectrometer to directly detect three microbially produced small molecule natural products, ectoine, prodigiosin, and tetracycline. Without requiring large quantities of microbial cultures and sample preparation, metabolites were directly detected in solids (i.e., TLC and agar plates) and liquids. The high flexibility and sensitivity of this technique is especially notable in light of the low cost of the OpenASAP system. Ectoine (143.0818 *m/z*, 1.76 ppm error), prodigiosin (324.2072 *m/z*, 1.19 ppm error), and tetracycline (445.1620 *m/z*, 2.04 ppm error) were successfully identified in *Arthrobacter* sp. strain FRX14, *M. frigida* strain DJPM01, and *S. alboflavus* (NRRL B-1273), respectively. (Figs. 15–17) In addition, the MS/MS spectra obtained for all three compounds in the microbial strains were consistent with the fragmentation patterns obtained from the standards (Figs. 15–17).

Sensitivity and analyte specific behavior

Sensitivity varied significantly for each compound, with an approximate limit of detention for ectoine being 10 pg/ml, prodigiosin at 10 ng/ml, and tetracycline at 100 ng/ml. Within the range of linear detector response R^2 was found to be between 0.958 and 0.997 for the compounds tested (Fig. 18). The sensitivity correlated with volatility and inversely correlated with molecular weight, which was unsurprising given our use of an atmospheric pressure chemical ionization (APCI) ionization source. The coefficient of variation with five replicate measurements of 10 μg/ml solutions was 0.113, 0.243, and 0.282 for ectoine, prodigiosin, and tetracycline, respectively. We found that the sampling volume was approximately 7.3 μl. (Fig. 19) which places the absolute limit of detection at 7 fg for ectoine, 7 pg for prodigiosin, and 70 pg for tetracycline. This sampling volume is high due to the relatively large surface area of the capillary that was immersed in standard solutions to generate standard curves and sampling volume calculations. Sampling of solids, trace materials, or microbial colonies may result in a lower sampling volume and thus require a higher concentration to meet the

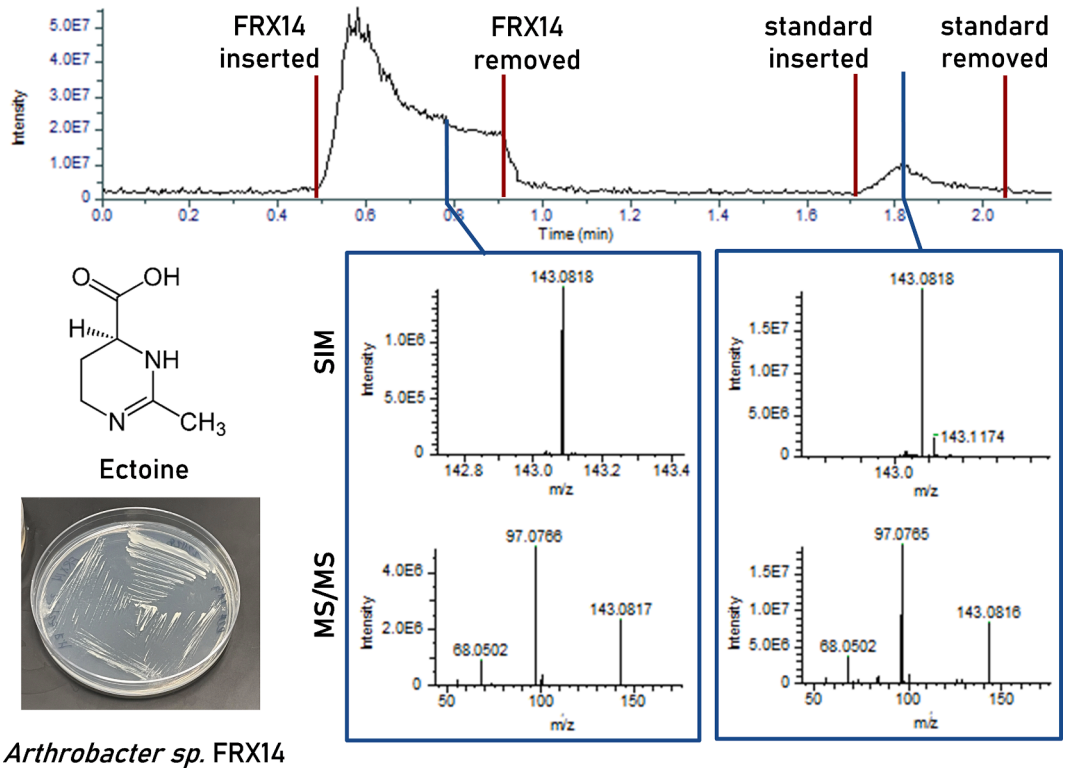

Fig. 15. ASAP data for sequential sampling of *Arthrobacter* sp. strain FRX14 and ectoine standard. SIM scan masses and matching MS/MS spectra for ectoine (143.0821 theoretical *m/z*) confirm its presence in FRX14.

absolute limit of detection for a given analyte. The relatively high variation among technical replicates as well as the possible variation in sampling volumes when using a capillary for sampling limits the precision of quantitation. Further study is needed to evaluate whether improvements are possible.

During heating of the high concentration tetracycline standards by the APCI source, formation of pyrrolized material was noted. Similarly, we found that ASAP is not suitable for peptidic analytes, such as desferrioxamine, which was observed to completely degrade (data not shown). Despite the observed pyrolysis of tetracycline at high concentrations the limit of detection is similar to that previously reported for quantitation of tetracycline on the QE HF-X in a traditional LC-MS workflow (20 ng/g in samples after extraction and concentration, the next concentration below 100 ng/ml used in this study was 10 ng/ml). [35].

By contrast, ectoine is very challenging to detect in environmental samples with LC-MS using conventional C18 stationary phases due to its high polarity (Fig. 20), but very easy using ASAP. The high polarity of ectoine is particularly problematic for samples that contain nonvolatile salts as ectoine may be lost during desalting with SPE cartridges, and the use of a divert valve to protect the mass spectrometer will also divert ectoine. (Fig. 20) In cases where analysis with a HILIC column is not possible or desirable, ASAP may be an attractive alternative. We observed a very large difference between the limits of detection (based on the presence of an integrable peak and S/N $>$ 10) and quantitation (based on the region of linearity). It is unclear why this behavior occurs. Adsorption of analytes to LC-MS vials is a well-known confounder in trace analyte analysis [36] and it is conceivable that a similar phenomenon occurs in which analytes are adsorbed and concentrated on the capillary until saturation of surface sites occurs at approximately 100 ng/ml for ectoine. If this is the case, then the effect may be advantageous for some applications. However, it should not be relied upon as adsorption may be matrix dependent.

The limits of detection and quantitation for prodigiosin appear to be similar as no integrable peak was present under 10 ng/ml and the detector response was linear over the entire concentration range tested with $R^2 > 0.99$. Interpretation of ASAP data may be complicated as no orthogonal separation method is employed, as such spectra can be complex. Thus, it may be more appropriately used in targeted workflows where standards are available. Prodigiosin was a notable exception to this as in both the standard and microbial sample *m/z* 324.2072 was the base peak in MS1 spectra; thus, we presented MS1 spectra obtained with a full scan method in Fig. 16. The mass of the prodigiosin analogue 2-methyl-3-butyl prodiginine (*m/z* 310.1915) is conspicuous in these spectra and we have previously documented the production of this compound by *M. frigida* strain DJPM01.[29].

TLC-MS with OpenASAP

TLC analysis (Fig. 21) revealed the presence of two red pigmented compounds, prodigiosin (*m/z* 324.2076, Rf 0.8) and another

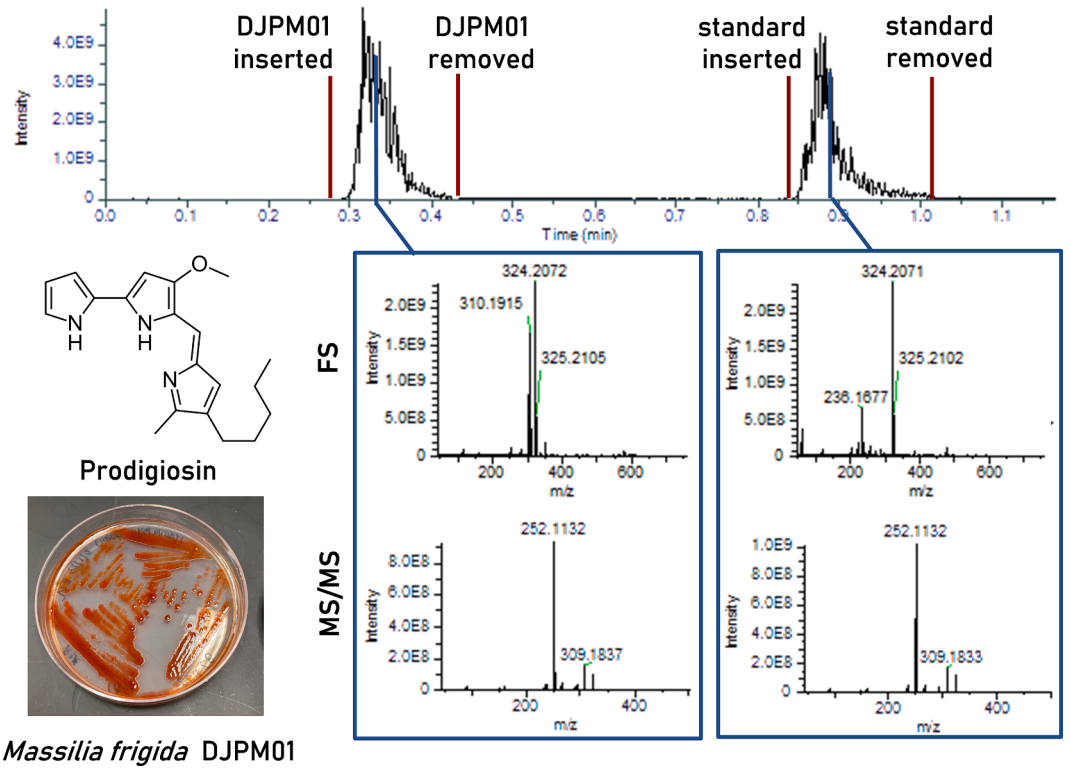

Fig. 16. ASAP data for sequential sampling of *M. frigida* strain DJPM01 and prodigiosin standard. MS1 full scan spectra and matching MS/MS spectra for prodigiosin (324.2075 theoretical *m/z*) confirm its presence in *M. frigida* strain DJMP01.

compound we have yet to conclusively identify (Rf 0.71), in the ethyl acetate extract of *M. frigida* strain DJPM01. Two other orange pigmented compounds were observed which likely represent short-lived decomposition intermediates as one was observed in the authentic standard. These proved very unstable on silica and likely in storage as they could not be observed when TLC was repeated. The Rf value of prodigiosin present in the microbial extract was identical to that of an authentic standard. Work to refine TLC plate sampling is ongoing.

OpenASAP applications and future directions

3D-printers are now common shared resources at academic institutions, enabling this technology to be more accessible. However, if such resources are not available, the system can be printed on even very low-cost consumer-grade 3D printers with the addition of an affordable hardened steel nozzle. We estimate that an investigator with no tools or consumables could reasonably purchase these and fabricate the system for under $200.

ASAP can facilitate the detection of compounds in complex sample matrices that are undetected by traditional ionization methods. As evidenced by our detection of ectoine, including directly from microbial colonies, which was not tractable using conventional LC-MS methods, the flexibility and high sensitivity of ASAP is desirable for its detection. This can be beneficial for analytical analyses of extreme environments, which are subject to extreme ranges of chemical and physical variables, including hypersaline ponds, metal contaminated sites, or locations with extreme pH [37]. These locales are considered to be edge cases in terms of analytical chemistry, where analytical methods may be more challenging or less thoroughly validated [37], and ASAP is useful for these applications as no specialized LC or sample preparation methods need to be employed. Although we validated the OpenASAP system on a high-resolution Orbitrap instrument, we have demonstrated that 3D-printed components can survive the demanding APCI environment and thus adaptation of this approach to develop peripherals for smaller field operable instruments is feasible.

ASAP has the potential to accelerate or enhance other techniques. The use of the OpenASAP system coupled with TLC to detect prodigiosin and another closely eluting compound in the ethyl acetate extract of *M. frigida* strain DJPM01 demonstrates the potential of this system for downstream processing of complex mixtures. TLC remains a widely used technique for separation of complex mixtures, [38] and the ability of OpenASAP to detect compounds of interest directly from the TLC plate can greatly expedite screening and analysis of these mixtures. Furthermore, the use of OpenASAP in bioassay-guided fractionation of natural products may be highly beneficial, particularly in conjunction with bioautography as bioactive TLC spots on a plate could be directly sampled to assign putative identifications during dereplication of known compounds. Similarly, the system can be used to monitor the products of synthetic reactions, where it can quickly identify the presence and purity of target compounds, eliminating the need for time-consuming

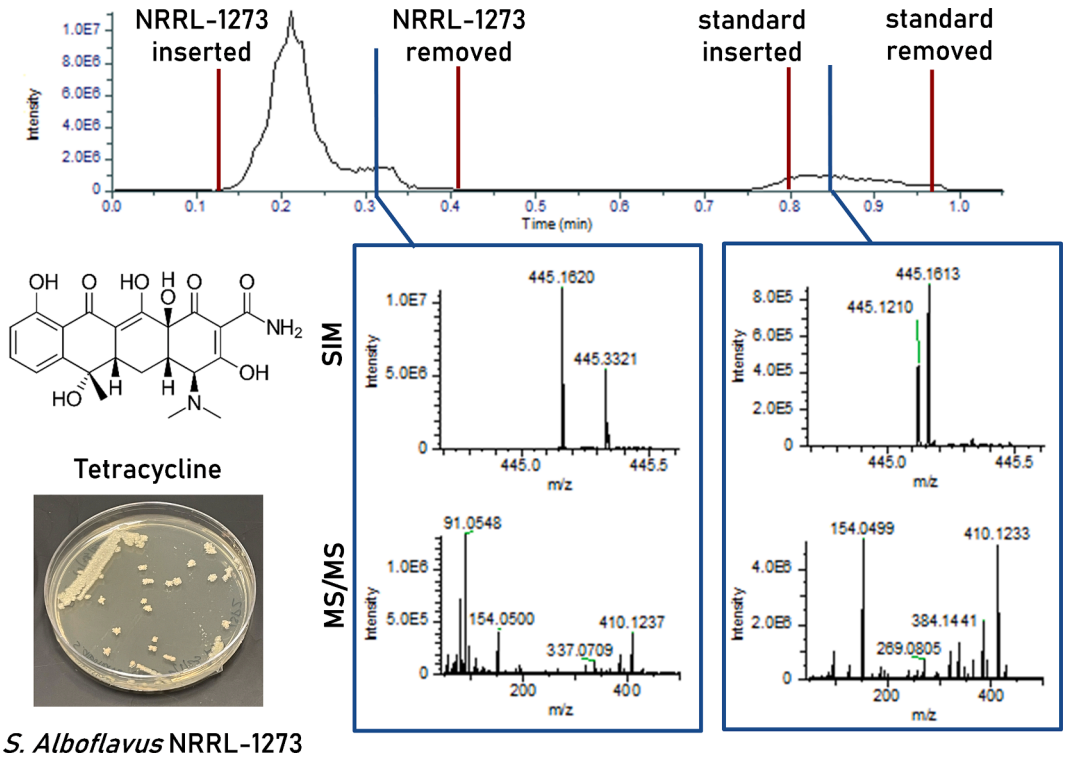

Fig. 17. ASAP data for sequential sampling of *S. alboflavus* NRRL B-1273 and tetracycline standard. SIM scan masses and the presence of numerous key fragments MS/MS spectra for tetracycline (445.161093 theoretical *m/z*) confirm its presence in *S. alboflavus* NRRL B-1273. Additional fragments are present in the MS/MS spectra and these are likely due to the presence of isobaric compounds. Use of a multiple reaction monitoring method may be desirable in such cases.

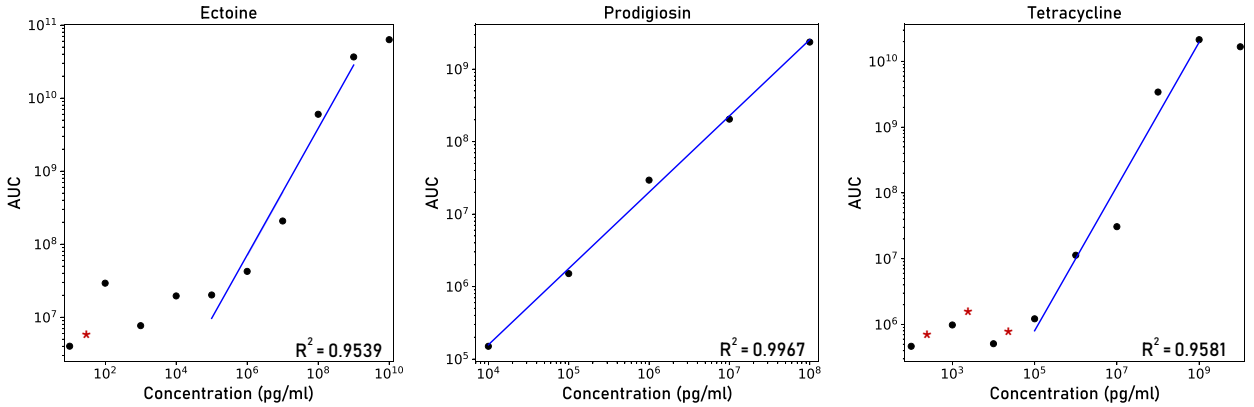

Fig. 18. Standard curves for the natural product standards tested. Data points marked with red asterisks were below the limit of detection (S/N 10 threshold). R^2 values were calculated over the approximate range of linearity, 10^5-10^9 pg/ml for ectoine, 10^4-10^8 pg/ml for prodigiosin, and 10^5-10^9 pg/ml for tetracycline. (For interpretation of the references to colour in this figure legend, the reader is referred to the web version of this article.)

purification steps.

While ASAP has many advantages, researchers should be cognizant of the low stability of some compound classes under APCI ionization conditions. Future studies could adapt ASAP to ionization sources more appropriate for larger compounds or those with poor thermal stability, such as desorption electrospray ionization (DESI), [39] dielectric barrier discharge ionization (DBDI), [40] or low temperature plasma ionization (LTP). [20].

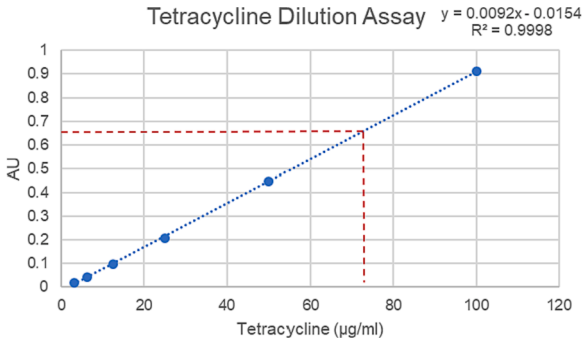

Fig. 19. Standard curve of tetracycline solutions based on absorbance at 300 nm with the red lines denoting the absorbance and concentration of a 10 mg/ml solution of tetracycline sampled with the OpenASAP system, and then dispersed into 1 ml methanol. The final concentration of 73 µg/ml indicates a 137-fold dilution from the 10 mg/ml stock and thus a sampled volume of 7.3 µl. (For interpretation of the references to colour in this figure legend, the reader is referred to the web version of this article.)

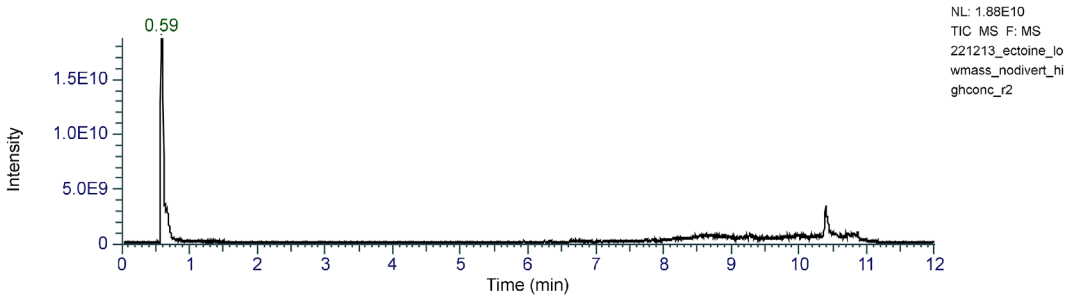

Fig. 20. LC-MS Total Ion Chromatogram (TIC) of the ectoine standard using the methods described in Shaffer et al. (2023) [29]. Ectoine elutes within the solvent front at 0.59 min due to its high polarity. Analysis of microbial cultures like those used in this study would not be possible as a divert valve would need to be employed to divert salts in the solvent from contaminating the mass spectrometer.

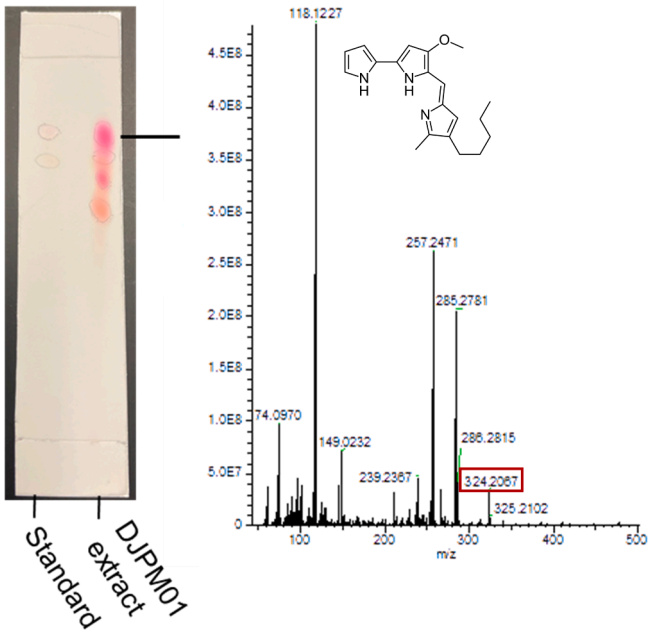

Fig. 21. TLC plate spotted with an ethyl acetate extract of *M. frigida* strain DJPM01 and prodigiosin standard, and the corresponding MS1 spectra obtained from conducting ASAP on the prodigiosin spot.

Conclusions

The OpenASAP system increases the accessibility of affordable, ambient ionization and sampling techniques to researchers. While we have validated this system to detect low-abundance secondary metabolites in microbial cultures, OpenASAP can be used in many other applications as ASAP and other ambient ionization techniques, such as DART, have been used in diagnostic medicine, forensic science, chemical ecology, and for environmental monitoring. The lack of solvents and noble gasses required for operation make the OpenASAP system an attractive option for mass spectrometry in remote locations where resources are limited. Future studies could further optimize the OpenASAP system for different applications and investigate its potential use in field testing, where a small linear ion trap instrument, a portable nitrogen concentrator, and an ASAP system could be utilized. Overall, the OpenASAP system presents a promising, inexpensive platform for the rapid and sensitive detection of a wide range of analytes in various fields.

CRediT authorship contribution statement

Robert Samples: Conceptualization, Methodology, Visualization, Investigation, Writing – original draft. **Riko Mukoyama:** Investigation. **Jacob Shaffer:** Resources. **Jill Mikucki:** Resources, Funding acquisition. **Lesley-Ann Giddings:** Investigation, Writing – original draft, Funding acquisition.

Declaration of Competing Interest

The authors declare that they have no known competing financial interests or personal relationships that could have appeared to influence the work reported in this paper.

Acknowledgments

We are grateful for the assistance of Eric Jensen, Director of the Center for Design and Fabrication at Smith College, for assistance with fabrication of the ASAP probe.

Funding

This work was supported by the National Science Foundation Office of Polar Programs [#2148730 to JAM and #2148731 to L-AG].

References:

[1] C. Li, S. Chu, S. Tan, X. Yin, Y. Jiang, X. Dai, X. Gong, X. Fang, D. Tian, Towards higher sensitivity of mass spectrometry: a perspective from the mass analyzers, Front. Chem. 9 (2021), https://doi.org/10.3389/fchem.2021.813359.
[2] R.M. Smith, Before the injection—modern methods of sample preparation for separation techniques, J. Chromatogr. a. 1000 (2003) 3–27, https://doi.org/10.1016/S0021-9673(03)00511-9.
[3] B. Cañas, C. Piñeiro, E. Calvo, D. López-Ferrer, J.M. Gallardo, Trends in sample preparation for classical and second generation proteomics, J. Chromatogr. a. 1153 (2007) 235–258, https://doi.org/10.1016/j.chroma.2007.01.045.
[4] T.M. Annesley, Ion Suppression in Mass Spectrometry, Clin. Chem. 49 (2003) 1041–1044, https://doi.org/10.1373/49.7.1041.
[5] T.-H. Kuo, E.P. Dutkiewicz, J. Pei, C.-C. Hsu, Ambient ionization mass spectrometry today and tomorrow: embracing challenges and opportunities, Anal. Chem. 92 (2020) 2353–2363, https://doi.org/10.1021/acs.analchem.9b05454.
[6] E.A. Bruns, V. Perraud, J. Greaves, B.J. Finlayson-Pitts, Atmospheric solids analysis probe mass spectrometry: a new approach for airborne particle analysis, Anal. Chem. 82 (2010) 5922–5927, https://doi.org/10.1021/ac101028j.
[7] Library Details | Waters. https://www.waters.com/nextgen/us/en/library/library-details.html?documentid=720003907&t=waters-ASAPApplicationNotebook-720003907 (accessed July 14, 2023).
[8] J. Osorio, M. Aznar, C. Nerín, C. Elliott, O. Chevallier, Comparison of LC-ESI, DART, and ASAP for the analysis of oligomers migration from biopolymer food packaging materials in food (simulants), Anal. Bioanal. Chem. 414 (2022) 1335–1345, https://doi.org/10.1007/s00216-021-03755-0.
[9] Contractor Information Summary - New York OGS. https://online.ogs.ny.gov/purchase/spg/pdfdocs/3870022962ContractorInfo.pdf (accessed July 14, 2023).
[10] Atmospheric Solids Analysis Probe (ASAP) | Waters. https://www.waters.com/nextgen/us/en/services/instrument-services/instrument-upgrades/mass-spectrometry-ms-upgrades/atmospheric-solids-analysis-probe.html (accessed July 14, 2023).
[11] ASAP® Probe. https://www.ionsense.com/Products/ASAP_Probe (accessed July 14, 2023).
[12] M. Grajewski, M. Hermann, R.D. Oleschuk, E. Verpoorte, G.I.J. Salentijn, Leveraging 3D printing to enhance mass spectrometry: a review, Anal. Chim. Acta. 1166 (2021), 338332, https://doi.org/10.1016/j.aca.2021.338332.
[13] C. Drees, S. Höving, W. Vautz, J. Franzke, S. Brandt, 3D-printing of a complete modular ion mobility spectrometer, Mater. Today. 44 (2021) 58–68, https://doi.org/10.1016/j.mattod.2020.10.033.
[14] A. Hollerbach, P.W. Fedick, R.G. Cooks, Ion mobility-mass spectrometry using a dual-gated 3D printed ion mobility spectrometer, Anal. Chem. 90 (2018) 13265–13272, https://doi.org/10.1021/acs.analchem.8b02209.
[15] B.C. Hauck, B.R. Ruprecht, P.C. Riley, Accurate and on-demand chemical sensors: A print-in-place ion mobility spectrometer, Sens. Actuators B Chem. 362 (2022), 131791, https://doi.org/10.1016/j.snb.2022.131791.
[16] N.S. García-Rojas, H. Guillén-Alonso, S. Martínez-Jarquín, A. Moreno-Pedraza, L.D. Soto-Rodríguez, R. Winkler, Build, share and remix: 3d printing for speeding up the innovation cycles in ambient ionisation mass spectrometry (AIMS), Metabolites 12 (2022) 185, https://doi.org/10.3390/metabo12020185.
[17] G.I.J. Salentijn, R.D. Oleschuk, E. Verpoorte, 3D-printed paper spray ionization cartridge with integrated desolvation feature and ion optics, Anal. Chem. 89 (2017) 11419–11426, https://doi.org/10.1021/acs.analchem.7b02490.
[18] H.M. Brown, P.W. Fedick, Rapid, low-cost, and in-situ analysis of per- and polyfluoroalkyl substances in soils and sediments by ambient 3D-printed cone spray ionization mass spectrometry, Chemosphere 272 (2021), 129708, https://doi.org/10.1016/j.chemosphere.2021.129708.
[19] H.M. Brown, T.J. McDaniel, K.R. Doppalapudi, C.C. Mulligan, P.W. Fedick, Rapid, in situ detection of chemical warfare agent simulants and hydrolysis products in bulk soils by low-cost 3D-printed cone spray ionization mass spectrometry, Analyst 146 (2021) 3127–3136, https://doi.org/10.1039/D1AN00255D.

[20] S. Martínez-Jarquín, A. Moreno-Pedraza, H. Guillén-Alonso, R. Winkler, Template for 3D printing a low-temperature plasma probe, Anal. Chem. 88 (2016) 6976–6980, https://doi.org/10.1021/acs.analchem.6b01019.
[21] Q. Liu, S. Martínez-Jarquín, W. Ge, R. Zenobi, Development of a 3D-printed ionization source for single-cell analysis, Anal. Chem. 95 (2023) 1823–1828, https://doi.org/10.1021/acs.analchem.2c04279.
[22] J.-B. Hu, T.-R. Chen, C.-H. Chang, J.-Y. Cheng, Y.-C. Chen, P.L. Urban, A compact 3D-printed interface for coupling open digital microchips with Venturi easy ambient sonic-spray ionization mass spectrometry, Analyst 140 (2015) 1495–1501, https://doi.org/10.1039/C4AN02220C.
[23] K.J. Zemaitis, T.D. Wood, Integration of 3D-printing for a desorption electrospray ionization source for mass spectrometry, Rev. Sci. Instrum. 91 (2020), 104102, https://doi.org/10.1063/5.0004626.
[24] N.S. García-Rojas, A. Moreno-Pedraza, I. Rosas-Román, E. Ramírez-Chávez, J. Molina-Torres, R. Winkler, Mass spectrometry imaging of thin-layer chromatography plates using laser desorption/low-temperature plasma ionisation, Analyst 145 (2020) 3885–3891, https://doi.org/10.1039/D0AN00446D.
[25] C. McEwen, S. Gutteridge, Analysis of the inhibition of the ergosterol pathway in fungi using the atmospheric solids analysis probe (ASAP) method, J. Am. Soc. Mass Spectrom. 18 (2007) 1274–1278, https://doi.org/10.1016/j.jasms.2007.03.032.
[26] ASAP Atmospheric Solids Analysis Probe - Advion X Interchim, Advion. https://www.advion.com/products/asap/ (accessed July 15, 2023).
[27] RADIAN ASAP Direct Mass Detector | Waters. https://www.waters.com/waters/en_US/RADIAN-ASAP-Direct-Mass-Detector/nav.htm?cid=135073413&locale=en_US (accessed September 20, 2023).
[28] S. Bhandari, R.A. Lopez-Anido, D.J. Gardner, Enhancing the interlayer tensile strength of 3D printed short carbon fiber reinforced PETG and PLA composites via annealing, Addit. Manuf. 30 (2019), 100922, https://doi.org/10.1016/j.addma.2019.100922.
[29] J.M.C. Shaffer, L.-A. Giddings, R.M. Samples, J.A. Mikucki, Genomic and phenotypic characterization of a red-pigmented strain of *Massilia frigida* isolated from an Antarctic microbial mat, accessed July 15, 2023, Front. Microbiol. 14 (2023), https://doi.org/10.3389/fmicb.2023.1156033.
[30] J.M.C. Shaffer, L.-A. Giddings, R.M. Samples, J.A. Mikucki, B.A. Ball, R.A. Virginia. "Molecular indicators of environmental change in an Antarctic Polar Desert." In 2023 XIII Scientific Committee on Antarctic Research Biology Symposium, 2023.
[31] D. Vijay, N.S. Alshamsi, Z. Moussa, M.K. Akhtar, Extraction of the anticancer and antimicrobial agent, prodigiosin, from Vibrio gazogenes PB1 and its identification by 1D and 2D NMR, Molecules 27 (2022) 6030, https://doi.org/10.3390/molecules27186030.
[32] B. Zakeri, G.D. Wright, Chemical biology of tetracycline antibiotics, Biochem. Cell Biol. 86 (2008) 124–136, https://doi.org/10.1139/O08-002.
[33] A.E. Asagbra, A.I. Sanni, O.B. Oyewole, Solid-state fermentation production of tetracycline by Streptomyces strains using some agricultural wastes as substrate, World J. Microbiol. Biotechnol. 21 (2005) 107–114, https://doi.org/10.1007/s11274-004-2778-z.
[34] M. Beaumesnil, A.L. Mendes Siqueira, M. Hubert-Roux, C. Loutelier-Bourhis, C. Afonso, A. Racaud, Y. Bai, High-performance thin-layer chromatography with atmospheric solids analysis probe mass spectrometry for analysis of gasoline polymeric additives, Rapid Commun. Mass Spectrom. 34 (2020) e8755.
[35] W. Zhao, R. Jiang, W. Guo, C. Guo, S. Li, J. Wang, S. Wang, Y. Li, Screening and analysis of multiclass veterinary drug residues in animal source foods using UPLC-Q-Exactive Orbitrap/MS, Bull. Environ. Contam. Toxicol. 107 (2021) 228–238, https://doi.org/10.1007/s00128-021-03273-w.
[36] Y. Huang, Y. Hu, E.M. Yuill, A.S. Marriott, J. Chadwick, J. Li, J. Zang, S.A. Miller, Circumventing glass vial and diluent effects on solution stability of small molecule analytes during analytical method development and validation, J. Pharm. Biomed. Anal. 213 (2022), 114676, https://doi.org/10.1016/j.jpba.2022.114676.
[37] L.-A. Giddings, D.J. Newman, Bioactive compounds from extremophiles, in: L.-A. Giddings, D.J. Newman (Eds.), Bioactive Compounds from Extremophiles: Genomic Studies, Biosynthetic Gene Clusters, and New Dereplication Methods, Springer International Publishing, Cham, 2015, https://doi.org/10.1007/978-3-319-14836-6_1.
[38] A. Ahmad Dar, P. Sangwan, A. Kumar, Chromatography: An important tool for drug discovery, J. Sep. Sci. 43 (2020) 105–119, https://doi.org/10.1002/jssc.201900656.
[39] J. Tillner, V. Wu, E.A. Jones, S.D. Pringle, T. Karancsi, A. Dannhorn, K. Veselkov, J.S. McKenzie, Z. Takats, Faster, more reproducible DESI-MS for biological tissue imaging, J. Am. Soc. Mass Spectrom. 28 (2017) 2090–2098, https://doi.org/10.1007/s13361-017-1714-z.
[40] N. Na, M. Zhao, S. Zhang, C. Yang, X. Zhang, Development of a dielectric barrier discharge ion source for ambient mass spectrometry, J. Am. Soc. Mass Spectrom. 18 (2007) 1859–1862, https://doi.org/10.1016/j.jasms.2007.07.027.